FGFR2-Amplified Gastric Cancer Cell Lines Require FGFR2 and Erbb3 Signaling for Growth and Survival

Kaiko Kunii,[1] Lenora Davis,[2] Julie Gorenstein,[3] Harold Hatch,[2] Masakazu Yashiro,[4] Alessandra Di Bacco,[1] Cem Elbi,[3] and Bart Lutterbach[2]

[1]Pharmacology, [2]Cancer Biology and Therapeutics, and [3]Cancer Pathways, Merck Research Laboratories, Boston, Massachusetts; and [4]Department of Surgical Oncology, Osaka City University Graduate School of Medicine, Osaka, Japan

Abstract

We have identified a critical role for amplified *FGFR2* in gastric cancer cell proliferation and survival. In a panel of gastric cancer cell lines, fibroblast growth factor receptor 2 (FGFR2) was overexpressed and tyrosine phosphorylated selectively in *FGFR2*-amplified cell lines KatoIII, Snu16, and OCUM-2M. FGFR2 kinase inhibition by a specific small-molecule inhibitor resulted in selective and potent growth inhibition in *FGFR2*-amplified cell lines, resulting in growth arrest in KatoIII cells and prominent induction of apoptosis in both Snu16 and OCUM-2M cells. *FGFR2*-amplified cell lines also contained elevated phosphotyrosine in EGFR, Her2, and Erbb3, but the elevated phosphorylation in EGFR could not be inhibited by gefitinib or erlotinib. We show that the elevated EGFR, Her2, and Erbb3 phosphotyrosine is dependent on FGFR2, revealing EGFR family kinases to be downstream targets of amplified *FGFR2*. Moreover, shRNA to Erbb3 resulted in a loss of proliferation, confirming a functional role for the activated EGFR signaling pathway. These results reveal that both the FGFR2 and EGFR family signaling pathways are activated in *FGFR2*-amplified gastric cancer cell lines to drive cell proliferation and survival. Inhibitors of FGFR2 or Erbb3 signaling may have therapeutic efficacy in the subset of gastric cancers containing *FGFR2* amplification. [Cancer Res 2008;68(7):2340–8]

Introduction

Gastric cancer is second to lung cancer as the most lethal cancer worldwide (1) and can be classified as a well-differentiated intestinal subtype or as a poorly differentiated diffuse subtype (2). Whereas overall gastric cancer incidence has declined, the incidence remains high in Asian countries including Japan, Korea, and China (1, 3). Diffuse gastric cancer is associated with a less favorable prognosis relative to the intestinal subtype, but for gastric cancer overall, the prognosis is poor, with 5-year survival rates in the range of 10% to 15% (4, 5). An exception to this poor survival is observed in clinical practice in Japan, where a combination of screening and aggressive surgical intervention has resulted in 5-year survival rates approaching 60% (4, 6). Despite these efforts, late-stage gastric cancer continues to have a dismal prognosis, and thus there remains an urgent need for improved therapy.

Multiple oncogenic alterations have been described in gastric cancer. These include a relatively low incidence of *ras* mutations (7, 8), loss-of-function mutations in the E-cadherin gene *CDH1* (9), as well as amplification of receptor tyrosine kinases *Her2, Met*, and *FGFR2* (10–12). Interestingly, these alterations are associated with specific subtypes of gastric cancer. Whereas *Her2* amplification (13) and *ras* mutations (14, 15) are found in the well-differentiated intestinal subtype, *CDH1* mutation as well as *Met* and *FGFR2* amplification occurs more frequently in the undifferentiated diffuse subtype (9, 12, 16, 17). Interestingly, in an analysis of matched primary and metastatic tumor samples, *FGFR2* amplification in some cases occurred only in a metastatic lesion, suggesting a role for this kinase in the development of metastases (18).

Fibroblast growth factor receptor 2 (FGFR2) is a member of the FGFR receptor tyrosine kinase family, which consists of 4 receptors and 23 ligands (19). Ligand binding leads to FGFR2 dimerization, autophosphorylation, and activation of signaling components including Akt and Erk kinases. FGFR2 was originally identified as an amplified DNA sequence from the gastric cancer cell line KatoIII (18, 20), and subsequent efforts identified *FGFR2* amplification in 3% to 10% of primary gastric cancers (12, 16, 21). A role for FGFR2 in cancer is supported by the observation that transgenic expression of the FGFR2-specific ligand FGF7 (KGF) leads to prostate hyperplasia and mammary adenocarcinoma (22). In addition, activating mutations in *FGFR2* have been described in primary gastric cancer (23). Despite these observations, a role for FGFR2 in oncogenesis has not been widely accepted, and evidence also exists that FGFR2 is down-regulated and may have a growth suppressive role in some cancers (24). As well, with regard to *FGFR2* amplification, it remained unclear whether *FGFR2* or neighboring genes in the 10q26 locus were contributing factors for gastric cell transformation. Recent work using multikinase small-molecule inhibitors has provided evidence that in cell lines expressing FGFR2, the kinase can be required for cancer cell proliferation (25, 26). However, the small-molecule inhibitors used in these studies inhibit multiple kinases in addition to FGFR2, raising the possibility that inhibition of a combination of kinases is required for growth inhibition.

We used both a highly specific FGFR inhibitory small molecule and FGFR2 shRNA to define a critical role for *FGFR2* amplification in gastric cancer cell growth. In KatoIII, Snu16, and OCUM-2M cell lines, *FGFR2* amplification results in a highly overexpressed and constitutively phosphorylated receptor. FGFR2 inhibition by shRNA or a small-molecule inhibitor induced potent and selective growth inhibition and apoptosis in these cell lines. Interestingly, elevated tyrosine phosphorylation in epidermal growth factor receptor (EGFR), Erbb3, and Her2 was found in *FGFR2*-amplified cell lines. This elevated phosphorylation was resistant to inhibition by either gefitinib or erlotinib but was abrogated on FGFR2 kinase inhibition, revealing EGFR family members to be downstream

Note: Supplementary data for this article are available at Cancer Research Online (http://cancerres.aacrjournals.org/).

Requests for reprints: Bart Lutterbach, Cancer Biology and Therapeutics, BMB 10-122, Merck Research Laboratories, 33 Avenue Louis Pasteur, Boston, MA 02115. Phone: 617-992-2038; Fax: 617-992-2412; E-mail: bart_lutterbach@merck.com.

doi:10.1158/0008-5472.CAN-07-5229

components of FGFR2 signaling in *FGFR2*-amplified cell lines. shRNA inhibition of Erbb3 inhibited growth in *FGFR2*-amplified lines, and thus the FGFR2-mediated activation of Erbb3 is essential for proliferation. We conclude that the activated FGFR2 kinase in *FGFR2*-amplified gastric cancer cells stimulates proliferation and survival through activation of multiple signaling pathways including a novel transactivation of EGFR family members. As well, our results suggest that FGFR2 inhibition may have therapeutic efficacy in the subset of poorly differentiated gastric cancers containing *FGFR2* amplification.

Materials and Methods

Cell lines. KatoIII, Snu16, AGS, 23132/87, Snu1, N87, MKN45, and Snu5 were from American Type Culture Collection. NUGC4, OCUM-1, and IM95 were from the Health Science Research Resources Bank (Japan Health Sciences Foundation). Cells were maintained in RPMI plus 10% FCS and 100 μg/mL penicillin-strep (Sigma). IM95 medium contained 10 mg/L insulin. GTL-16 cells were a gift from S. Giordano and P.M. Comoglio (University of Torino Medical School, Torino, Italy). OCUM-2M cells were from Osaka City University (Osaka, Japan).

Quantitative PCR analysis of *FGFR2* genomic amplification. Genomic DNA was purified with the DNeasy kit protocol per manufacturer's instructions (Qiagen). Primers and probe used for FGFR2 qPCR are listed 5′ to 3′: F-CCCCCTCCACAATCATTCCT, R-ACCGGCGGCCTAGAAAAC, and VIC-TCGTCTAGCCTTTTCTTTT-MGBNFQ. Primers and probe for single-copy reference gene RNase P were from Applied Biosystems, as was TaqMan Universal PCR reagent mix (4324018). Reactions were done in quadruplicate with genomic DNA at 2.5 ng, primers at 900 nmol/L, and probes at 250 nmol/L under standard thermocycling conditions (2 min at 50°C, 10 min at 95°C, 40 cycles of 15 s at 95°C, and 1 min at 60°C). Data were normalized to RNase P and then to the calibrator sample (normal stomach genomic DNA, BioChain Institute D1234248).

Fluorescence *in situ* hybridization analysis. KatoIII gastric carcinoma cells were treated with colcemid at 0.02 μg/mL for 3 h and DNA fluorescence *in situ* hybridization (FISH) was done as previously described (27, 28) using bacterial artificial chromosome clones RP11-62L18 and RP11-20J15 containing FGFR2 as probes. Probes were directly labeled using Spectrum Orange dUTP and Spectrum Green dUTP (Abbott Molecular, Inc.).

shRNA production and infection. shRNA sequences were F1, GCCAACCTCTCGAACAGTATTCAAGAGATACTGTTCGAGAGGTTGGC; F2, GGACTTGGTGTCATGCACCTTCAAGAGAGGTGCATGACACCAAGTCC; F3, GGACTGTAGACAGTGAAACTTCAAGAGAGTTTCACTGTCTACAGTCC; F4, GAGATTGAGGTTCTCTATATTCAAGAGATATAGAGAACCTCAATCTC; luciferase, CACCGGTGTTGTAACAATATCGACGAATCGATATTGTTACAA-CACCAAA; and scrambled, CACCGTCTCCACGCGCAGTACATTTC-GAAAAATGTACTGCGCGTGGAGACAAAA. Oligos were annealed and 5′ *Bbs*I and 3′ *Spe*I used to clone into a proprietary ENTR plasmid (mouse U6 promoter) followed by conversion to Plenti6/Block-iT-DEST (Invitrogen) using Gateway (Invitrogen). Erbb3 shRNAs in PLKO-1 from Open Biosystems were E8, RHS3979-9630819; E9, RHS3979-9630819; and E10, RHS3979-9630819. Controls from Sigma included SHC001, a vector control, and SHC002, a PLKO-1 nontargeting control that activates the RNA-induced silencing complex and the RNAi pathway but does not target a human transcript. Virus production and titer determination were as directed by the supplier. Lentiviral infection was at a multiplicity of infection of 10 to 20. For growth analysis, cells were seeded at 4,000 per well in 96-well plates, whereas for Western blot analysis cells were seeded at 40,000 per well in 12-well plates. Viral supernatants were added for 20 h in the presence of 8 μg/mL polybrene, at which point viral supernatants were removed and replaced with growth medium containing 10% fetal bovine serum.

Compound treatment of cell lines. A 10 mmol/L solution of PD173074 (Sigma) was diluted in DMSO in a 96-well plate to create a dilution series of compound at 1,000× concentration: 100, 40, 20, 10, 5, and 2 μmol/L. Two microliters of each stock solution were removed to separate wells using a multichannel pipettor and diluted with 200 μL of DMEM/0.5% FCS. Finally, 11 μL of this dilution were added to triplicate wells containing target cells in 100-μL growth medium. After 3 d, cell numbers were quantitated using the Vialight reagent (Vialight assay kit, Cambrex). For some assays, independent analysis by cell counting on a hematocytometer confirmed the results of Vialight. Luminescence was quantified with a Topcount NXT HTS (Perkin-Elmer) and IC_{50} determinations made by using logistic four-parameter curve fitting. For quantitation of phosphotyrosine in FGFR2 and EGFR family members, blots were scanned and quantitated using ImageQuant software. Values corresponding to band intensity were plotted against drug concentration to establish an IC_{50} of drug inhibition. Gefitinib and erlotinib were purchased from the Beth Israel Hospital pharmacy. Profiling of 224 independent kinases was done through the KinaseProfiler service at Upstate Biotechnologies.

Western blotting, immunoprecipitation, antibodies, and growth factors. Lysates were prepared in 30 mmol/L Tris-HCl (pH 7.5), 50 mmol/L NaCl, 5 mmol/L EDTA, 50 mmol/L NaF, 30 mmol/L NaPPi, 1% Triton X-100, 0.5% Igepal, 10% glycerol, 1 mmol/L vanadate, 1 mmol/L bpPhen (Calbiochem), and protease inhibitor (Roche), and Western blotting and immunoprecipitation were as described (29, 30). The following antibodies were from R&D Systems: FGFR2 (MAB6841), phospho-FGFR2 (AF3285), EGFR (AF231), Her2 (AF1129), Erbb3 (AF234), and Erbb4 (AF1131). Antibodies from Cell Signaling Technology were FGFR2 (sc-122), phospho-FGFR2 (3471), Y1289 Erbb3 (4791), Y845 EGFR (2231), AKT (9272), pAKT 473 (4058), extracellular signal–regulated kinase (Erk; 9102), pErk (4370), poly(ADP-ribose) polymerase (PARP; 9542), and β-actin (4967) antibodies. Y1173 EGFR antibody was from Biosource Invitrogen. Anti–glyceraldehyde-3-phosphate dehydrogenase (GAPDH) was from Fitzgerald Industries. 4G10 phosphotyrosine antibody was from Upstate. Recombinant EGF and FGF7 were from R&D Systems.

Ras activation assays. Ras activation was assayed on 400-μg cell lysates with a ras activation kit (Upstate) according to kit procedures.

Flow cytometry. A Becton Dickinson FACSCalibur was used for flow cytometry on 500,000 cells. Nonadherent cells were included in the analysis. Cells were fixed overnight in 1-mL ice cold 70% ethanol, then washed in PBS and stained with propidium iodide/RNase (BD PharMingen) for 3 h. ModFit software was used to determine relative distribution in G_1, S, and G_2-M, and manual gating to determine sub-G_1 content.

Receptor tyrosine kinase array. Array 001 was from R&D Systems and was used according to the supplier's protocols as previously described (29). Fifty micrograms of cell lysates were used for the experiments.

Sequencing. Ras isoform and FGFR2 sequencing was done at Transgenomic Labs.

Results

FGFR2 is overexpressed and activated in *FGFR2*-amplified cell lines. We assembled a panel of 10 gastric cancer cell lines and investigated FGFR2 expression and activation in relationship to *FGFR2* genomic amplification. KatoIII, Snu16, and OCUM-2M have been reported to contain elevated FGFR2 gene copy (12, 31, 32). To confirm this result, we developed a quantitative genomic PCR assay that identified high-level *FGFR2* gene copy in KatoIII, OCUM-2M, and Snu16 cells (Fig. 1*A*). Next, we determined the genomic amplification status of *FGFR2* in KatoIII cells by FISH analysis using *FGFR2* and chromosome 10 centromeric region specific probes. FISH analysis revealed prominent clustered, large *FGFR2* signals consistent with homogeneous staining regions in both metaphase and interphase nuclei of KatoIII cells (Supplementary Fig. S1, *arrowheads*). This high-level *FGFR2* amplification was distinct from the endogenous *FGFR2* gene locus, suggesting a targeted amplification of this locus (Supplementary Fig. S1, *arrow*).

We next confirmed that *FGFR2*-amplified KatoIII, OCUM-2M, and Snu16 cell lines expressed high levels of FGFR2 protein (Fig. 1*B*). Both KatoIII and OCUM-2M express COOH-terminally

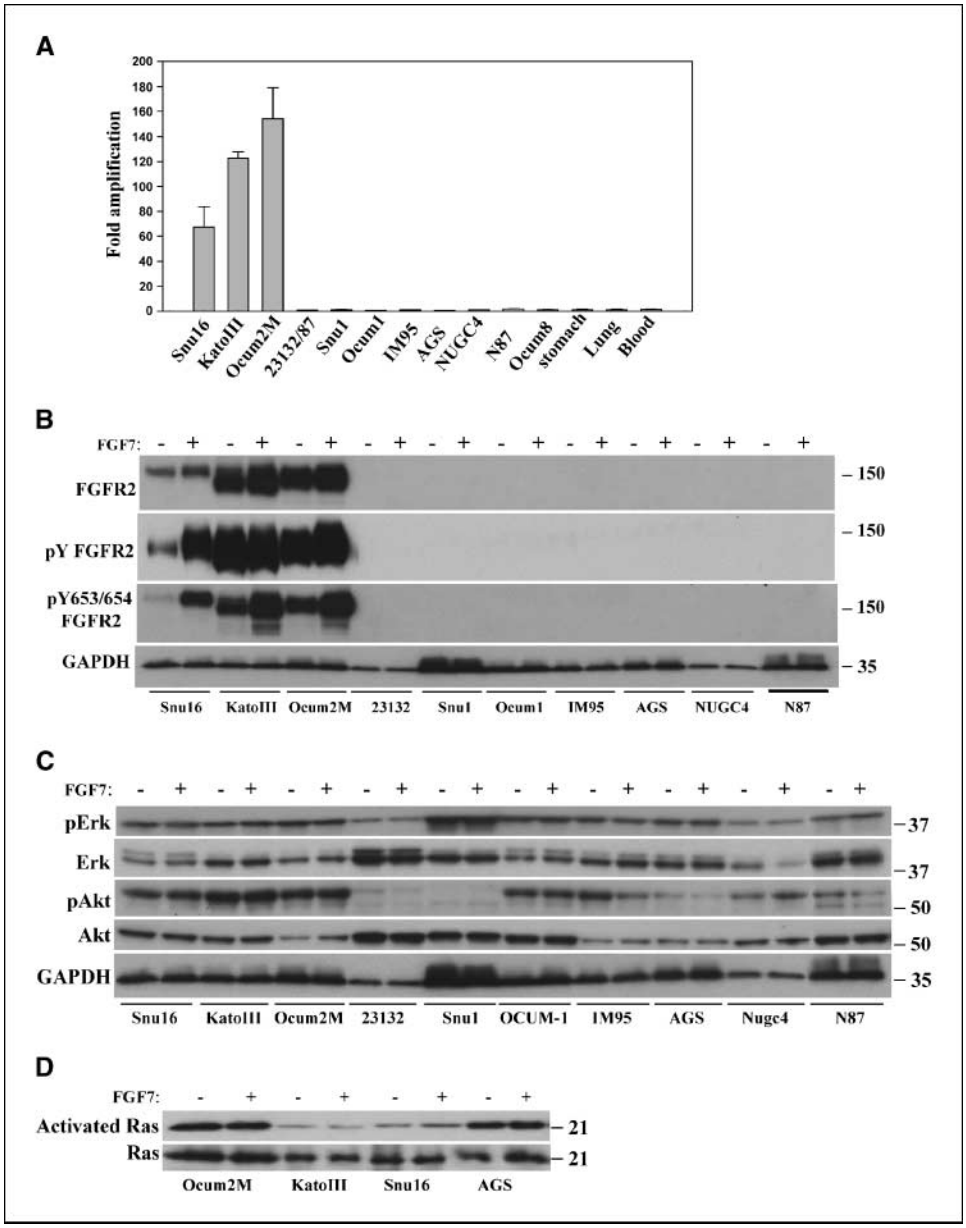

Figure 1. *FGFR2* amplification leads to FGFR2 overexpression and activation in Snu16, KatoIII, and Ocum2M cells and results in activated downstream signaling. *A, FGFR2* is highly amplified in Snu16, KatoIII, and Ocum2M cell lines. Quantitative PCR was done on genomic DNA from the indicated cell lines as described in Materials and Methods. RNase P was used as an internal reference and signals were standardized to normal stomach DNA. *B,* cells (5×10^5) in six-well plates were untreated (−) or treated (+) with FGF7 (100 ng/mL, 5 min) and 60-μg protein lysate (prepared according to Materials and Methods) was subjected to SDS-PAGE and Western blotting with antibodies recognizing FGFR2, FGFR2 activation loop phosphorylation Y653/654, and GAPDH. For phospho-tyrosine detection, lysates were first immunoprecipitated with MAB6841 as described in Materials and Methods, separated by SDS-PAGE, and Western blotted for phosphotyrosine with the 4G10 antibody. *C* and *D,* downstream signaling is activated in KatoIII, Snu16, and Ocum2M cells. *C,* lysates used in *B* were analyzed by Western blotting for the indicated phosphorylated or total proteins. *D,* Ras activation was done on separate samples as described in Materials and Methods. Representative of three experiments. (OCUM-2M was abbreviated to Ocum2M in the figures for space considerations.)

truncated splice variants resulting in the lower molecular weight kinase in these cells relative to Snu16 (32). Consistent with a truncation in the COOH terminus, a FGFR2 COOH-terminal reactive antibody (sc-122) does not detect FGFR2 from KatoIII and OCUM-2M cells, but does detect FGFR2 from Snu16 cells (data not shown). We similarly found very low expression of FGFR2 in the *Met*-amplified cell lines MKN45, GTL-16, SNU5, and HS746T (data not shown).

High basal levels of FGFR2 activation site phosphorylation were found in the cell lines overexpressing FGFR2, although both KatoIII and OCUM-2M contained higher basal activation relative to Snu16 (Fig. 1*B*). The basal phosphorylation was further stimulated by FGF7 in Snu16 cells, but only marginally in KatoIII and OCUM-2M. Because the Y653/654 phosphospecific FGFR antibody cross-reacts with FGFR1, FGFR3, and FGFR4 (data not shown), we tested the FGFR2 activation status by FGFR2 immunoprecipitation and phosphotyrosine detection with 4G10. Consistent with elevated activation site phosphorylation, Fig. 1*B* reveals that total phosphotyrosine is highly elevated in the FGFR2-overexpressing cell lines. Similar to the Y653/654 site, total FGFR2 tyrosine phosphorylation is significantly stimulated by FGF7 addition only in the Snu16 cell line. However, the basal phosphorylation of Akt and Erk in Snu16 cells was not stimulated by FGF7 (Fig. 1*C*), suggesting that basal FGFR2 activation is sufficient to activate the mitogenic signaling pathways in this cell line. As well, the lack of Akt and Erk activation by FGF7 in the nonamplified cell lines is consistent with the undetectable levels of FGFR2 in these lines (Fig. 1*B*). *Ras* was also found to be activated in *FGFR2*-amplified cells, and again FGF7 did not result in further activation in Snu16 (Fig. 1*D*). Interestingly, *ras* activation in *FGFR2*-amplified cell lines can be similar to levels seen in the *ras* mutant AGS and Snu1 cells (Fig. 1*D* and Supplementary Fig. S2). Also of note, sequencing revealed that *ras* isoforms are wild-type in KatoIII, Snu16 (33), and OCUM-2M cells

(data not shown), and thus *ras* activation is likely a result of constitutive receptor signaling.

To address the mechanism of FGFR2 activation, we determined if the high basal phosphorylation in FGFR2 was due to activating mutations described in craniofacial syndromes as well as in a subset of primary gastric cancer (23, 34). However, complete sequencing of *FGFR2* in KatoIII, Snu16, and OCUM-2M did not reveal mutations (data not shown). Finally, conditioned media from KatoIII or OCUM-2M cell lines did not activate FGFR2 phosphorylation in Snu16 (data not shown). Thus, the observed FGFR2 activation is likely due to dimerization as a result of receptor overexpression.

FGFR2 kinase activity is required for proliferation of *FGFR2*-amplified cell lines. Although FGFR2 is highly activated, it remained to be determined if FGFR2 kinase activity is required for gastric cancer cell growth. A Merck multikinase inhibitor compound in clinical development[5] inhibited multiple serine/threonine and tyrosine kinases (including FGFR2) and inhibited the growth of *FGFR2*-amplified gastric cancer cell lines (data not shown). However, it was not clear whether a combined inhibition of multiple kinases was required for growth inhibition or whether specific FGFR2 inhibition alone was sufficient. Therefore, we used the FGFR-selective inhibitor PD173074 for further experiments (35). This compound was found to inhibit FGFR kinases *in vitro* at an IC_{50} of 3.6 nmol/L for FGFR1, 3.3 nmol/L for FGFR2, and 5.3 nmol/L for FGFR3 (data not shown). To confirm selectivity for FGFR, we found that this compound significantly inhibited only FGFR1, FGFR2, and FGFR3 (but not FGFR4) of 224 kinases tested (Supplementary Fig. S3). We note that inhibition of the CAMKIIγ isoform was not linear.

Having established PD173074 as a potent and selective inhibitor of FGFR activity *in vitro*, we found that this compound also potently inhibited FGFR2 phosphorylation in cells (Fig. 2*A*), with IC_{50} values from 7 to 13 nmol/L (Fig. 2*B*). PD173074 inhibition of FGFR2 phosphorylation was correlated with a strikingly potent and selective growth inhibition in the *FGFR2*-amplified cell lines (Fig. 2*B*). The average IC_{50} for growth inhibition of three *FGFR2*-amplified lines was 18 nmol/L, whereas the average for 10 nonamplified lines was 4,200 nmol/L, a difference of >200-fold in potency. Importantly, the similar IC_{50} for biochemical inhibition of FGFR2 phosphorylation and growth inhibition strongly implicates FGFR2 phosphorylation as the activity required for cell growth. These results reveal that the overexpressed and highly activated FGFR2 kinase is the key driver of proliferation in *FGFR2*-amplified cell lines.

We were interested to determine if the *FGFR2*-amplified cell lines might be nonspecifically sensitive to a variety of receptor tyrosine kinase or chemotherapeutic inhibitors. However, gefitinib and erlotinib were not potent growth inhibitors of *FGFR2*-amplified cell lines, with IC_{50} values ranging from 6,000 to 8,500 nmol/L in KatoIII cells (Supplementary Fig. S4), and combination treatment of PD173074 and gefitinib did not improve the potency of either compound treatment alone (data not shown). Gefitinib function was confirmed by inhibition of the NUGC4 cell line at an IC_{50} of 125 nmol/L (data not shown), similar to previously reported inhibition (36). Regarding chemotherapeutic compounds, paclitaxel and 5-fluorouracil had relatively similar potency against *FGFR2*-amplified cells in comparison with non–*FGFR2*-amplified cells (Supplementary Fig. S5).

FGFR2 shRNA inhibits cell growth. Although PD173074 is highly selective for FGFR1, FGFR2, and FGFR3, we additionally treated cells with shRNA directed to FGFR2 to confirm its role in cell growth. We infected *FGFR2*-amplified cell lines with FGFR2 shRNA using lentiviral vectors and achieved efficient FGFR2 knockdown in OCUM-2M and KatoIII cells with shRNAs F2 and F3, but not with F1 and F4 (Fig. 3*A*). By contrast, we were unable to decrease FGFR2 protein in Snu16 cells. Using lentivirally expressed green fluorescent protein, we found that Snu16 cells were not efficiently infected even at much higher multiplicity of infection

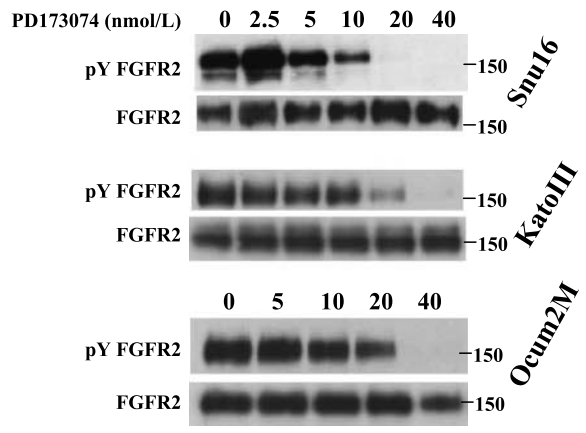

B

	IC_{50}(SD) (nmol/L)	
	Growth	FGFR2 pTyr
KatoIII	**12 (4)**	**13 (8)**
Ocum2M	**26 (9)**	**12 (5)**
Snu16	**20 (5)**	**7 (4)**
23132/87	1,750 (478)	
Ocum1	6,500 (707)	
IM95	5,250 (1,061)	
AGS	4,000 (283)	
N87	3,900 (566)	
Snu1	4,800 (1,697)	
Nugc4	9,500 (890)	
Gtl-16	4,250 (961)	
Snu5	3,850 (212)	

Figure 2. PD173074 inhibits FGFR2 phosphorylation and selectively inhibits growth of *FGFR2*-amplified cell lines. *A,* PD173074 inhibits FGFR2 phosphorylation. Cells were treated for 1 h with a titration of PD173074 (in nanomolar) as described in Materials and Methods. Lysates were prepared and 150 μg of protein were immunoprecipitated with MAB6841, separated on SDS-PAGE, and blotted for phosphotyrosine with 4G10. The blot was stripped and reprobed for total FGFR2. The experiment was repeated thrice with similar results. *B,* PD173074 inhibits cell growth. Cell lines were plated at 4,000 cells per well and incubated overnight. Cell lines were treated with a titration of PD173074 (in nanomolar) as described in Materials and Methods; after 3 d, relative cell numbers were determined with Vialight reagent. The IC_{50} values for growth inhibition are listed with SD and are results from four separate experiments. Also listed are the IC_{50} values (in nanomolar) for FGFR2 phosphotyrosine inhibition as determined by quantitation of data in *A* using ImageQuant software as described in Materials Methods. We note that only Ocum2M, Snu16, and KatoIII cells contain measurable FGFR2 phosphorylation.

[5] C. Dinsmore et al., in preparation.

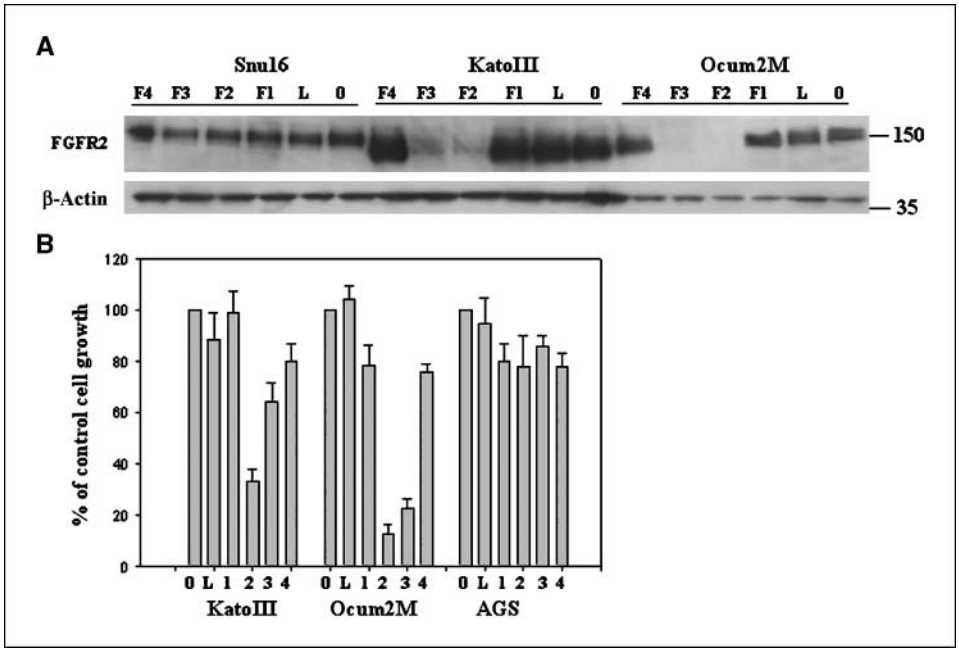

Figure 3. FGFR2 shRNA decreases FGFR2 protein levels and inhibits growth of KatoIII and Ocum2M cells. FGFR2 protein down-regulation by shRNA inhibits growth. *A,* cells were treated with four shRNAs targeting FGFR2 (*F1–F4*) or luciferase (*L*), or were untreated (*0*), as described in Materials and Methods. Western blotting for FGFR2 was done with MAB6841. *B,* cell growth after treatment with shRNA. Vialight reagent was used to measure relative cell growth. *Columns,* average percent inhibition relative to untreated cells from three independent experiments; *bars,* SD.

(data not shown). In OCUM-2M and KatoIII cells, FGFR2 knockdown by F2 and F3 was accompanied by growth inhibition, whereas the F1 and F4 shRNAs and a luciferase shRNA were not growth inhibitory (Fig. 3*B*). The non–*FGFR2*-amplified cell line AGS was not growth inhibited with F1, F2, F3, F4, and luciferase shRNAs. To address the poor infectivity of Snu16 cells, we selected for stable expression of FGFR2 shRNA with blasticidin. Stable lines could be established with all FGFR2 shRNA constructs, but Western blotting revealed no decrease in FGFR2 protein (data not shown), and thus shRNA treatment was uninformative for FGFR2 function in Snu16 cells. However, KatoIII and OCUM-2M show growth inhibition with F2 and F3 shRNAs, confirming the inhibition seen with PD173074.

***FGFR2*-amplified cell lines undergo growth arrest or apoptosis after inhibition of FGFR2.** To understand the mechanisms of growth inhibition in PD173074-treated cells, we analyzed the cell cycle distribution in KatoIII, OCUM-2M, and Snu16 by flow cytometry. Cells were treated with 100 nmol/L

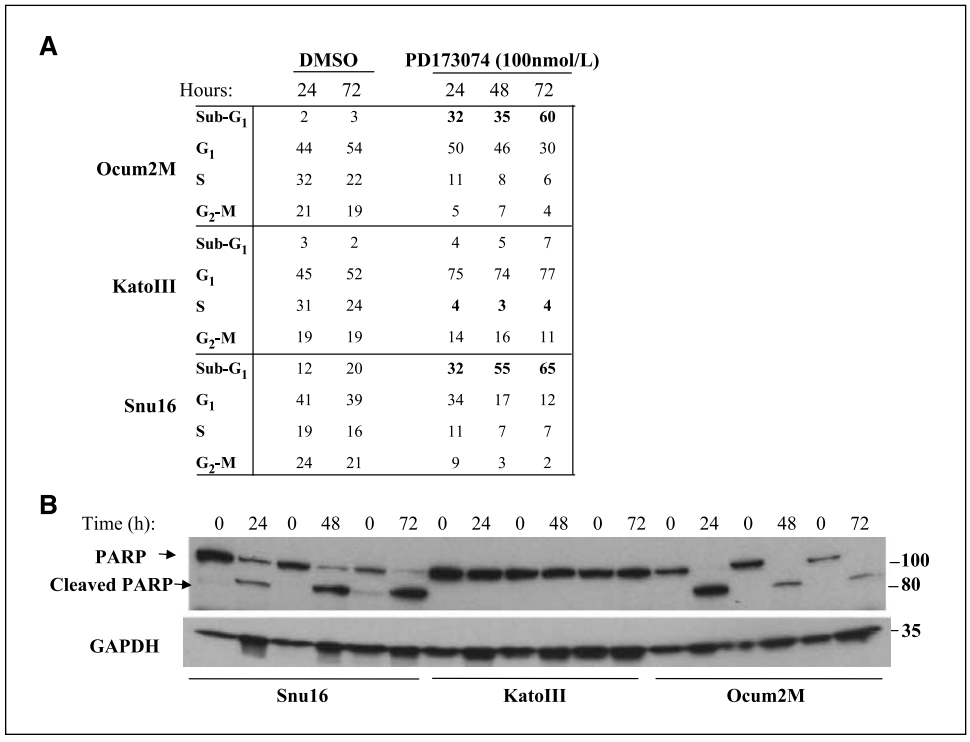

Figure 4. PD173074 results in a loss of S phase in KatoIII and apoptosis in Ocum2M and Snu16 cells. *A,* cell cycle profile of drug-treated cells. KatoII, Snu16, and Ocum2M cells (1×10^6) treated with 100 nmol/L PD173074 or DMSO at the indicated time points were processed for propidium iodide staining and fluorescence-activated cell sorting analysis as described in Materials and Methods. Tabular representation of cell cycle profiles as determined by ModFit software. *B,* duplicate cells treated as in *A* were isolated at the indicated time points and lysed for Western blotting analysis with cleaved PARP. β-Actin was used as a loading control (*bottom*). The position of full-length and cleaved PARP is indicated. Representative of two independent experiments.

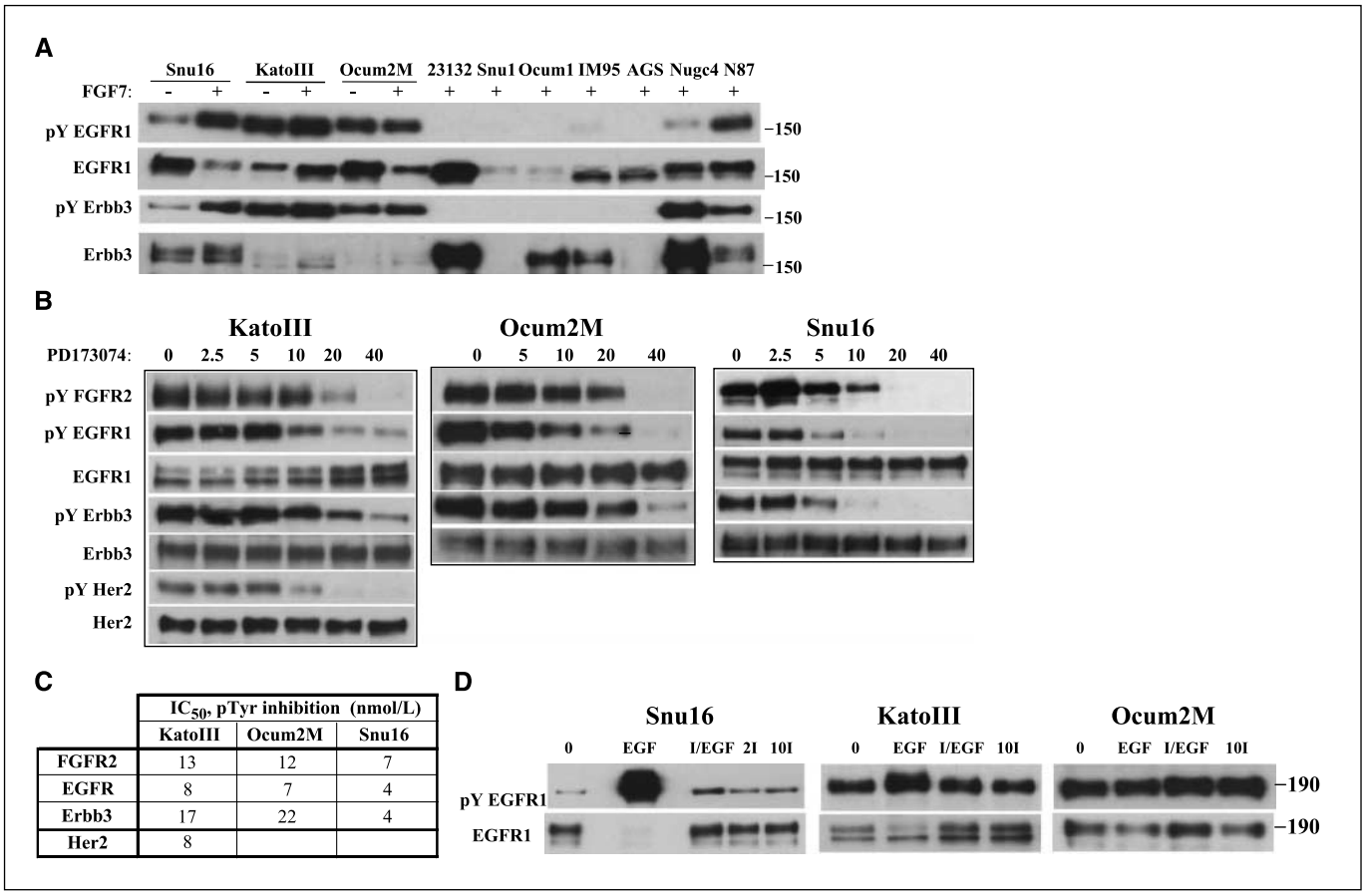

C

	IC_{50}, pTyr inhibition (nmol/L)		
	KatoIII	Ocum2M	Snu16
FGFR2	13	12	7
EGFR	8	7	4
Erbb3	17	22	4
Her2	8		

Figure 5. EGFR family tyrosine phosphorylation is elevated in *FGFR2*-amplified cell lines and is resistant to gefitinib but sensitive to FGFR2 inhibition. *A,* the indicated cell lysates (200 μg) were immunoprecipitated as described in Materials and Methods and probed for total tyrosine phosphorylation with 4G10. After stripping, total protein levels were detected with EGFR and Erbb3 antibodies. *B,* 200-μg lysates used in Fig. 3 were immunoprecipitated with antibodies to EGFR, Her2, or Erbb3, followed by washing, SDS-PAGE, Western blotting, and detection with 4G10 or total antibodies as described in Materials and Methods. *C,* IC_{50} (nmol/L) for inhibition of EGFR family phosphotyrosine obtained by quantitation of data in *B* with ImageQuant software. *D,* cells were either treated with EGF for 10 min (*EGF*) or pretreated with 2 μmol/L gefitinib (Iressa) for 1 h before EGF addition (*I/EGF*), or treated directly with 2 or 10 μmol/L of gefitinib for 2 h (*2I* and *10I*, respectively). After treatment, lysates were prepared and 200-μg protein was immunoprecipitated with the EGFR antibody AF231. Immunoprecipitates were subjected to SDS-PAGE and Western blotting and probed for phosphotyrosine. Representative of two experiments.

PD173074, and cell cycle distribution was analyzed at 24, 48, and 72 hours after drug addition. In all cell lines, 24 hours of drug treatment resulted in a strong (3- to 4-fold) decrease in S phase (Fig. 4*A*). In addition, both OCUM-2M and Snu16 revealed a 4-fold increase in the sub-G_1 cell population. This sub-G_1 fraction, which is suggestive of apoptosis, increased further by 72 hours to include >50% of the cell population (Fig. 4*A*). By contrast, even at the 72-hour time point, KatoIII cells had only a minor sub-G_1 population. Visual inspection of Snu16 and OCUM-2M cells after 72 hours of drug treatment revealed a profound loss of cell integrity in OCUM-2M and Snu16 cells, whereas KatoIII cells remained intact (Supplementary Fig. S6 and data not shown). Treatment of OCUM-2M with shRNAs F2 and F3 also resulted in a similar loss of cell integrity (data not shown). As a further test for apoptosis, we probed for cleaved PARP, a marker of caspase activation associated with apoptosis (Fig. 4*B*). Prominent induction of cleaved PARP could be seen as early as 24 hours after addition of PD173074 in both Snu16 and OCUM-2M cells. By contrast, KatoIII cells showed no induction of cleaved PARP, consistent with flow cytometry results. Thus, FGFR2 inhibition can result in dramatically different growth arrest phenotypes.

The growth suppression resulting from FGFR2 inhibition was likely due to loss of multiple signaling pathways after inhibitor treatment. To test this, we analyzed Erk and Akt phosphorylation as well as activation of *ras* after treatment of cell lines with PD173074 (Supplementary Fig. S7). Erk and Akt phosphorylation and *ras* activation were blocked in KatoIII, OCUM-2M, and Snu16 cells at increasing drug concentrations after 2 hours of treatment. Akt has been reported to become reactivated after EGFR inhibitor treatment of *Her2*-amplified cells at later time points (37). However, Akt phosphorylation remained inhibited in KatoIII cells at 48 and 72 hours of treatment with 40 and 100 nmol/L of PD173074 (data not shown). Whereas *ras* activity remained elevated in KatoIII cells after 2 hours of drug treatment (Supplementary Fig. S7), at 6 and 24 hours, loss of *ras* activation was similar to that seen in Snu16 and OCUM-2M cells (data not shown).

FGFR2 activates EGFR family members in *FGFR2*-amplified cell lines. *Met* amplification in lung and gastric cancer cell lines results in activation of EGFR family members (29, 30). A receptor tyrosine kinase array revealed that *FGFR2*-amplified lines also contain activated EGFR family members (Supplementary Fig. S8). We immunoprecipitated EGFR and Erbb3 from our cell line panel

and probed for phosphotyrosine (Fig. 5*A*), confirming activated EGFR and Erbb3 in *FGFR2*-amplified cell lines as well as in *Her2*-amplified (N87) or gefitinib-sensitive (NUGC4) cell lines. Interestingly, EGFR and Erbb3 tyrosine phosphorylation was elevated similarly in *FGFR2*-amplified cells and the *Her2*-amplified cell line N87. Using EGFR phosphospecific antibodies, we found that the Y845 activation site is constitutively phosphorylated, whereas the Y1173 docking site remains ligand inducible (data not shown). As well, Erbb3 Y1289 is phosphorylated in KatoIII and OCUM-2M, but not in Snu16 (data not shown). We tested Her2 activation and found that only KatoIII contained significant phosphotyrosine in Her2, whereas phosphotyrosine was not recovered from Erbb4 in any cell line (Fig. 5*B* and data not shown). A striking observation was that phosphorylation of Erbb3 and EGFR in Snu16 cells was stimulated by FGF7. Because FGF7 is a dedicated ligand for FGFR2 (19), this result suggested that FGF7 indirectly activated Erbb3 and EGFR via activation of FGFR2.

If EGFR family members are components of amplified *FGFR2* signaling, loss of FGFR2 would result in loss of EGFR family phosphorylation. This was confirmed as PD173074 treatment inhibited EGFR, Erbb3, and Her2 phosphorylation at concentrations similar to those required to inhibit FGFR2 phosphorylation (Fig. 5*B* and *C*). shRNA inhibition of FGFR2 also resulted in loss of Tyr^{1289} phosphorylation in Erbb3 (Supplementary Fig. S10). We conclude that EGFR family members are downstream targets of the amplified and highly activated FGFR2 kinase.

Erbb3 is required for proliferation of *FGFR2*-amplified cell lines. We treated cells with gefitinib to test EGFR function in *FGFR2*-amplified cell lines. Surprisingly, 10 μmol/L gefitinib did not inhibit basal EGFR phosphorylation in these three cell lines (Fig. 5*D*). Erlotinib at 10 μmol/L also failed to block EGFR phosphorylation (data not shown). Gefitinib activity was confirmed by its ability to block the dramatic EGF-mediated stimulation of EGFR in Snu16 cells (Fig. 5*D*, compare *lanes EGF* and *I/EGF*). As discussed above, gefitinib and erlotinib are poor inhibitors of KatoIII, OCUM-2M, and Snu16 proliferation, which is consistent with the observed lack of EGFR phosphorylation inhibition. Although EGFR was highly activated by EGF addition to Snu16 cells, both OCUM-2M and KatoIII had only a minor increase in EGFR phosphorylation, suggesting that the basal EGFR phosphorylation in KatoIII and OCUM-2M represents a near-maximal receptor activation.

Because gefitinib was unable to block EGFR phosphorylation, we tested a functional role for EGFR pathway activation in KatoIII, OCUM-2M, and NUGC4 cells using shRNA to Erbb3, a required partner for EGFR family signaling. Each of three shRNAs directed to Erbb3 resulted in efficient knockdown of Erbb3 protein (Fig. 6*A*). Growth of both KatoIII and OCUM-2M was inhibited by Erbb3 shRNA, but only minor growth inhibition was observed in the NUGC4 cell line, which also has highly activated Erbb3 (Fig. 6*B*).

Analysis of signaling after Erbb3 ablation revealed that both KatoIII and OCUM-2M have a loss of Akt Ser^{473} phosphorylation, consistent with known Erbb3 signaling through the Akt pathway (Fig. 6*A*). In OCUM-2M cells, both FGFR2 and Erk phosphorylation remained elevated after Erbb3 knockdown. Because Erbb3 shRNA did not induce cell death in OCUM-2M cells, as was observed with PD173074 treatment or FGFR2 knockdown (Fig. 6*B*, and data not shown), it is possible that signal transduction through activated Erk or FGFR2 accounts for survival in Erbb3-deficient OCUM-2M cells. In contrast to OCUM-2M, in KatoIII cells FGFR2 phosphorylation was reduced after Erbb3 knockdown, and this reduction was strongest with shRNA1 (Fig. 6*A*). As well, Erk phosphorylation was consistently inhibited with shRNA1. The FGFR2 phosphorylation that remains after shRNA2 and shRNA3 treatment may be sufficient to maintain Erk phosphorylation. The increased potency

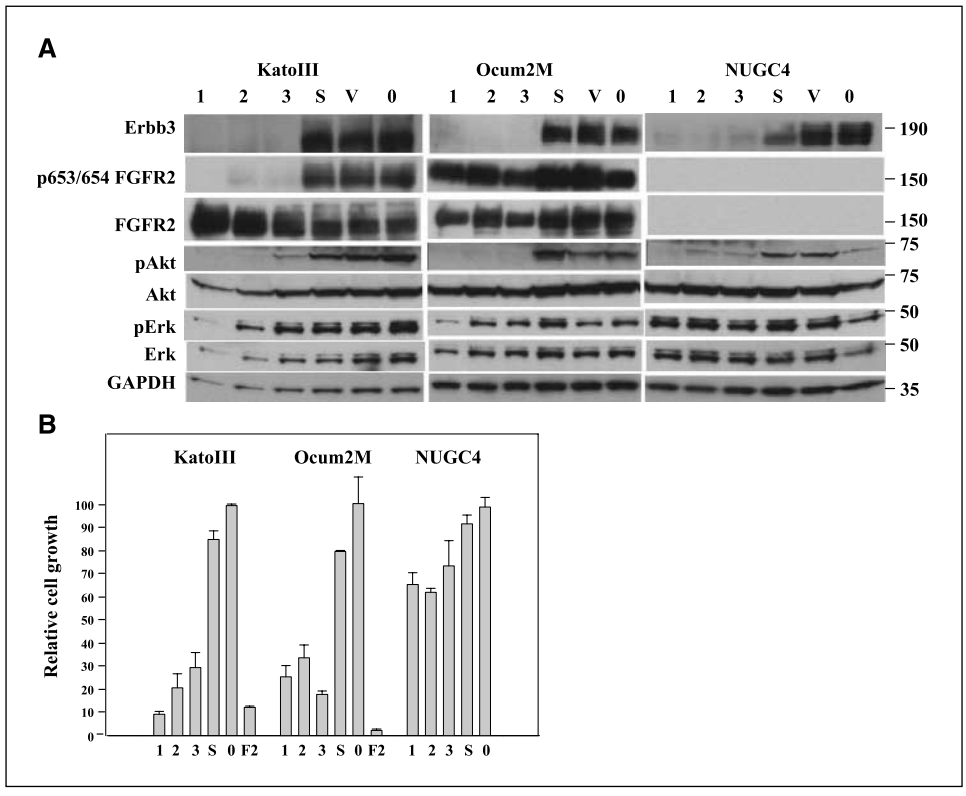

Figure 6. Erbb3 shRNA decreases Erbb3 protein levels and inhibits proliferation. *A,* the indicated cell lines were treated with three separate shRNAs directed to Erbb3 (*1, 2*, and *3*), a scrambled shRNA sequence (*S*), or vector (*V*), or left untreated (*0*), and were subjected to Western blotting 24 h after virus removal and probed for Erbb3, Y653/654 FGFR2, total FGFR2, Ser^{473} Akt (pAkt), Akt Thr^{202}, Tyr^{204} pErk, and Erk, with GAPDH as a loading control. Representative of two experiments. *B,* cells in 96-well plates were treated with the indicated shRNAs and allowed to grow for 6 d. Medium was replaced on day 3. Cell growth was quantitated from duplicate wells in three independent experiments and, using Vialight reagent and untreated control values, were normalized to 100% growth. F2 indicates that FGFR2 shRNA was included as a control for FGFR2 inhibition. *Columns,* average growth (percentage of untreated cell growth) from three experiments; *bars,* SD.

of shRNA1 to inhibit Erk and FGFR2 phosphorylation is currently not explained. As well, the molecular mechanism that results in reduction of FGFR2 phosphorylation in KatoIII cells relative OCUM-2M cells remains to be identified. However, we conclude that Erbb3 is a functional component of *FGFR2*-amplified cell growth.

Discussion

A key finding of this work is that *FGFR2*-amplified gastric cancer cell lines are dependent on the overexpressed and activated FGFR2 kinase for growth. Interestingly, in Snu16 and OCUM-2M cells, loss of FGFR2 resulted in apoptosis, whereas in KatoIII cells the loss of FGFR2 signaling resulted in growth arrest without apoptosis. Withdrawal of 100 nmol/L PD173074 from KatoIII cells after 7 days of treatment resulted in rapid outgrowth of cells (data not shown), confirming that compound-treated KatoIII cells are viable and capable of cell cycle reentry. In each of the *FGFR2*-amplified cell lines, there was a loss of Erk, Akt, and *ras* activation after FGFR2 inhibition. Recent work suggested that Akt may become reactivated at later time points following receptor tyrosine kinase inhibitor treatment, possibly contributing to drug resistance (37). However, Akt remained inhibited in KatoIII cells after 48 and 72 hours of PD173074 treatment, and thus the survival pathways that are active in KatoIII cells after FGFR2 inhibition remain to be identified.

A striking finding is that *FGFR2*-amplified cell lines contain elevated EGFR and Erbb3 phosphorylation (and in KatoIII cells, Erbb2 phosphorylation) that is dependent on FGFR2 kinase activity. Cross talk between FGFR2 and EGFR family kinases is also supported from our finding that the FGFR2-specific ligand FGF7 stimulated EGFR and Erbb3 phosphorylation in Snu16 cells. Importantly, EGF-stimulated phosphorylation of EGFR in Snu16 cells is not inhibited by PD173074 (Supplementary Fig. S9), and thus only the elevated basal phosphorylation in EGFR family members is FGFR2 dependent. Therefore, the dramatic phenotype associated with FGFR2 inhibition is a result of the combined loss of FGFR2 and EGFR family signaling.

shRNA inhibition of Erbb3 revealed that EGFR family signaling is required for cell growth in KatoIII and OCUM-2M cells. The FGFR2-EGFR interaction described here parallels recent reports that amplified Met can coactivate EGFR family signaling in lung cancer (29, 30). We find similar EGFR activation in *Met*-amplified gastric cancer cell lines (data not shown). Together these results reveal that *Met*- and *FGFR2*-amplified cell lines activate EGFR family proteins for cell transformation. The functional interaction between FGFR2 and EGFR family kinases could be mediated by a physical interaction, and thus we carried out coimmunprecipitation experiments in KatoIII, Snu16, and OCUM-2M cells. We used NH_2- and COOH-terminal antibodies under varying degrees of stringency, immunoprecipitating with either FGFR2 or Erbb3 and blotting for the converse protein. However, we were unable to show a specific interaction. Thus, a physical relationship between FGFR2 and Erbb3 remains to be identified.

The inability of gefitinib or erlotinib to block basal phosphorylation in EGFR is also consistent with a model in which amplified FGFR2 activates EGFR family members. FGFR2 is not inhibited by gefitinib and is therefore able to maintain elevated EGFR phosphorylation in the presence of gefitinib. This result also cautions against the use of phosphorylated EGFR to stratify gastric or lung cancer patients for EGFR small-molecule inhibitor therapy because, in a subset of these patients, EGFR is activated by FGFR2 or Met and will be resistant to EGFR inhibitor therapy. Furthermore, because Met amplification activates an EGFR signaling network that is resistant to gefitinib (29, 30), FGFR2 amplification may be yet another mechanism of clinical gefitinib resistance.

Because *Met*, *FGFR2*, and *Her2* amplification and *ras* mutations are exclusive of each other in gastric cancer cell lines, it is likely that each oncogene can independently activate transformed growth. The genetic defect in these cell lines can correlate with the specific inhibitor required to inhibit cancer cell growth. For example, *Met*-amplified cell lines SNU5, GTL-16, and MKN45 are insensitive to FGFR2 inhibition but are potently inhibited by Met inhibition (data not shown; ref. 38). Conversely, *FGFR2*-amplified cell lines are insensitive to Met-specific small-molecule inhibitors (data not shown) but are sensitive to FGFR2 inhibition. Finally, the NUGC4 (EGFR/Erbb3 activated; Fig. 6) and *Her2*-amplified N87 cell lines (39) are selectively inhibited by EGFR inhibitors or Herceptin, respectively (36, 40). It remains to be tested whether gastric cancers harboring these genetic alterations will be similarly responsive in a clinical setting. If this is the case, these studies along with those of others are beginning to define a rational treatment strategy for the subset of gastric cancers with activated/amplified receptor tyrosine kinases.

Acknowledgments

Received 9/7/2007; revised 1/2/2008; accepted 2/6/2008.

The costs of publication of this article were defrayed in part by the payment of page charges. This article must therefore be hereby marked *advertisement* in accordance with 18 U.S.C. Section 1734 solely to indicate this fact.

We thank Bo Pan and Wei Lu for discussions and Nancy Kohl and Victoria Richon for manuscript review; Chris Dinsmore, Jason Katz, Jonwon Lim, James Jewell, Kerrie Burgess, Michelle Machacek, Alan Northrup, David Guerin, and Jon Young for medicinal chemistry support; and M. Sekiguchi and J.G. Park for isolating the KatoIII and Snu16 cell lines, respectively.

References

1. Crew KD, Neugut AI. Epidemiology of gastric cancer. World J Gastroenterol 2006;12:354–62.
2. Lauren P. The two histological main types of gastric carcinoma: diffuse and so-called intestinal-type carcinoma. an attempt at a histo-clinical classification. Acta Pathol Microbiol Scand 1965;64:31–49.
3. Naylor GM, Gotoda T, Dixon M, et al. Why does Japan have a high incidence of gastric cancer? Comparison of gastritis between UK and Japanese patients. Gut 2006;55:1545–52.
4. Axon A. Symptoms and diagnosis of gastric cancer at early curable stage. Best Pract Res Clin Gastroenterol 2006;20:697–708.
5. Wanebo HJ, Kennedy BJ, Chmiel J, Steele G, Jr., Winchester D, Osteen R. Cancer of the stomach. A patient care study by the American College of Surgeons. Ann Surg 1993;218:583–92.
6. Inoue M, Tsugane S. Epidemiology of gastric cancer in Japan. Postgrad Med J 2005;81:419–24.
7. Lee KH, Lee JS, Suh C, et al. Clinicopathologic significance of the K-ras gene codon 12 point mutation in stomach cancer. An analysis of 140 cases. Cancer 1995;75:2794–801.
8. Arber N, Shapira I, Ratan J, et al. Activation of c-K-ras mutations in human gastrointestinal tumors. Gastroenterology 2000;118:1045–50.
9. Becker KF, Atkinson MJ, Reich U, et al. E-cadherin gene mutations provide clues to diffuse type gastric carcinomas. Cancer Res 1994;54:3845–52.
10. Houldsworth J, Cordon-Cardo C, Ladanyi M, Kelsen DP, Chaganti RS. Gene amplification in gastric and esophageal adenocarcinomas. Cancer Res 1990;50:6417–22.
11. Kuniyasu H, Yasui W, Kitadai Y, Yokozaki H, Ito H, Tahara E. Frequent amplification of the c-met gene in scirrhous type stomach cancer. Biochem Biophys Res Commun 1992;189:227–32.
12. Mor O, Ranzani GN, Ravia Y, et al. DNA amplification in human gastric carcinomas. Cancer Genet Cytogenet 1993;65:111–4.
13. Yokota J, Yamamoto T, Miyajima N, et al. Genetic alterations of the c-erbB-2 oncogene occur frequently in tubular adenocarcinoma of the stomach and are often accompanied by amplification of the v-erbA homologue. Oncogene 1988;2:283–7.
14. Yoo J, Park SY, Robinson RA, Kang SJ, Ahn WS, Kang CS. ras Gene mutations and expression of Ras signal

transduction mediators in gastric adenocarcinomas. Arch Pathol Lab Med 2002;126:1096–100.
15. Yashiro M, Nishioka N, Hirakawa K. K-ras mutation influences macroscopic features of gastric carcinoma. J Surg Res 2005;124:74–8.
16. Yoshida T, Sakamoto H, Terada M. Amplified genes in cancer in upper digestive tract. Semin Cancer Biol 1993; 4:33–40.
17. Tsujimoto H, Sugihara H, Hagiwara A, Hattori T. Amplification of growth factor receptor genes and DNA ploidy pattern in the progression of gastric cancer. Virchows Arch 1997;431:383–9.
18. Nakatani H, Sakamoto H, Yoshida T, et al. Isolation of an amplified DNA sequence in stomach cancer. Jpn J Cancer Res 1990;81:707–10.
19. Zhang X, Ibrahimi OA, Olsen SK, Umemori H, Mohammadi M, Ornitz DM. Receptor specificity of the fibroblast growth factor family. The complete mammalian FGF family. J Biol Chem 2006;281:15694–700.
20. Hattori Y, Odagiri H, Nakatani H, et al. K-sam, an amplified gene in stomach cancer, is a member of the heparin-binding growth factor receptor genes. Proc Natl Acad Sci U S A 1990;87:5983–7.
21. Hara T, Ooi A, Kobayashi M, Mai M, Yanagihara K, Nakanishi I. Amplification of c-myc, K-sam, and c-met in gastric cancers: detection by fluorescence *in situ* hybridization. Lab Invest 1998;78:1143–53.
22. Kitsberg DI, Leder P. Keratinocyte growth factor induces mammary and prostatic hyperplasia and mammary adenocarcinoma in transgenic mice. Oncogene 1996;13:2507–15.
23. Jang JH, Shin KH, Park JG. Mutations in fibroblast growth factor receptor 2 and fibroblast growth factor receptor 3 genes associated with human gastric and colorectal cancers. Cancer Res 2001;61:3541–3.
24. Bernard-Pierrot I, Ricol D, Cassidy A, et al. Inhibition of human bladder tumour cell growth by fibroblast growth factor receptor 2b is independent of its kinase activity. Involvement of the carboxy-terminal region of the receptor. Oncogene 2004;23:9201–11.
25. Takeda M, Arao T, Yokote H, et al. AZD2171 shows potent antitumor activity against gastric cancer overexpressing fibroblast growth factor receptor 2/keratinocyte growth factor receptor. Clin Cancer Res 2007;13: 3051–7.
26. Nakamura K, Yashiro M, Matsuoka T, et al. A novel molecular targeting compound as K-samII/FGF-R2 phosphorylation inhibitor, Ki23057, for scirrhous gastric cancer. Gastroenterology 2006;131: 1530–41.
27. Parada LA, McQueen PG, Munson PJ, Misteli T. Conservation of relative chromosome positioning in normal and cancer cells. Curr Biol 2002;12:1692–7.
28. Klokk TI, Kurys P, Elbi C, et al. Ligand-specific dynamics of the androgen receptor at its response element in living cells. Mol Cell Biol 2007;27:1823–43.
29. Lutterbach B, Zeng Q, Davis LJ, et al. Lung cancer cell lines harboring MET gene amplification are dependent on Met for growth and survival. Cancer Res 2007;67: 2081–8.
30. Engelman JA, Zejnullahu K, Mitsudomi T, et al. MET amplification leads to gefitinib resistance in lung cancer by activating ERBB3 signaling. Science 2007;316: 1039–43.
31. Dahlberg PS, Jacobson BA, Dahal G, et al. ERBB2 amplifications in esophageal adenocarcinoma. Ann Thorac Surg 2004;78:1790–800.
32. Ueda T, Sasaki H, Kuwahara Y, et al. Deletion of the carboxyl-terminal exons of K-sam/FGFR2 by short homology-mediated recombination, generating preferential expression of specific messenger RNAs. Cancer Res 1999;59:6080–6.
33. Kim IJ, Park JH, Kang HC, et al. Mutational analysis of BRAF and K-ras in gastric cancers: absence of BRAF mutations in gastric cancers. Hum Genet 2003; 114:118–20.
34. Reardon W, Winter RM, Rutland P, Pulleyn LJ, Jones BM, Malcolm S. Mutations in the fibroblast growth factor receptor 2 gene cause Crouzon syndrome. Nat Genet 1994;8:98–103.
35. Mohammadi M, Froum S, Hamby JM, et al. Crystal structure of an angiogenesis inhibitor bound to the FGF receptor tyrosine kinase domain. EMBO J 1998;17: 5896–904.
36. Namiki Y, Namiki T, Yoshida H, et al. Preclinical study of a "tailor-made" combination of NK4-expressing gene therapy and gefitinib (ZD1839, Iressatrade mark) for disseminated peritoneal scirrhous gastric cancer. Int J Cancer 2006;118:1545–55.
37. Sergina NV, Rausch M, Wang D, et al. Escape from HER-family tyrosine kinase inhibitor therapy by the kinase-inactive HER3. Nature 2007;445:437–41.
38. Smolen GA, Sordella R, Muir B, et al. Amplification of MET may identify a subset of cancers with extreme sensitivity to the selective tyrosine kinase inhibitor PHA-665752. Proc Natl Acad Sci U S A 2006;103:2316–21.
39. Kasprzyk PG, Song SU, Di Fiore PP, King CR. Therapy of an animal model of human gastric cancer using a combination of anti-erbB-2 monoclonal antibodies. Cancer Res 1992;52:2771–6.
40. Matsui Y, Inomata M, Tojigamori M, Sonoda K, Shiraishi N, Kitano S. Suppression of tumor growth in human gastric cancer with HER2 overexpression by an anti-HER2 antibody in a murine model. Int J Oncol 2005; 27:681–5.